

Design and Simulation of $\text{In}_x\text{Ga}_{1-x}\text{N}$ Based Solar Cells

A. BAKIRI^a, B. ZAIDI^{a,*}, K. AOUADJ^a,
S. GAGUI^b AND M.S. ULLAH^c

^a*Department of Physics, Faculty of Matter Sciences, LEPCM,
University of Batna 1, Batna, Algeria*

^b*Laboratory of Semiconductors, Department of Physics,
University of Badji-Mokhtar, Annaba, Algeria*

^c*Department of Electrical and Computer Engineering,
Florida Polytechnic University, Lakeland (FL) 33805, USA*

Received: 22.07.2020 & Accepted: 10.11.2020

Doi: [10.12693/APhysPolA.139.46](https://doi.org/10.12693/APhysPolA.139.46)

*e-mail: beddiaf.zaidi@univ-batna.dz

The aim of our work was to innovatively design and simulate an $\text{In}_x\text{Ga}_{1-x}\text{N}$ -based thin-film solar cell which is considered as a promising candidate for high performance solar cells. By inserting SnS, CdS and TCO layers, different cell parameters, such as the efficiency η , the fill factor FF, the current density J_{sc} , the open circuit voltage V_{oc} and the current-voltage (J - V) characteristics, of four configurations, specifically, $\text{In}_x\text{Ga}_{1-x}\text{N}/\text{SnS}/\text{ZnO}$, $\text{In}_x\text{Ga}_{1-x}\text{N}/\text{CdS}/\text{ZnO}$, $\text{In}_x\text{Ga}_{1-x}\text{N}/\text{In}_{0.5}\text{Ga}_{0.5}\text{N}/\text{ZnO}$ and $\text{In}_x\text{Ga}_{1-x}\text{N}/\text{SnS}/\text{TCO}$, were investigated. The influence of an SnS, $\text{In}_{0.5}\text{Ga}_{0.5}\text{N}$ and CdS buffer layer on the $\text{In}_x\text{Ga}_{1-x}\text{N}/\text{SnS}/\text{ZnO}$ structure and the effect of a TCO layer on the electrical characteristics of the structure were also investigated. It was revealed that the current density increases with the increase in the indium content, however, as the concentration attains a value of 80%, J_{cc} approximately becomes constant. The no-load voltage V_{oc} was observed to decrease as a function of the indium content (from 50 to 80%), however, it slightly increased for $\text{In}_{0.9}\text{Ga}_{0.1}\text{N}$ and for the binary compound InN . The computed results indicated that the effect of doping concentration and thickness of each layer on the electrical parameters of the $\text{In}_x\text{Ga}_{1-x}\text{N}$ alloys may result in enhancing the performance of solar cells.

topics: CdS, SnS, InGaN, IWO

1. Introduction

Recent studies have shown that semiconductors based on group-III nitrides have significant potential in the photovoltaic applications [1–5] and, among these, the $\text{In}_x\text{Ga}_{1-x}\text{N}$ alloy is a promising candidate for thin-film solar cells. This alloy exhibits potential photovoltaic properties, such as tolerance to radiation, high mobility, lifetimes of charge carriers as well as thermal and lattice matching. Furthermore, the $\text{In}_x\text{Ga}_{1-x}\text{N}$ material has an attractive tuneable bandgap (offering a very unique opportunity for designing) that varies from 0.7 to 3.42 eV and a high optical absorption coefficient (allowing for a thinner layer of material) over 10^5 cm^{-1} , indicating a better absorption of the solar spectrum [6]. Additionally, the layer of InGaN can be deposited by employing various techniques [7], such as metal organic chemical vapour deposition (MOCVD) [8], metal organic vapour phase epitaxy (MOVPE) and molecular beam epitaxy (MBE). These techniques make it possible to grow $\text{In}_x\text{Ga}_{1-x}\text{N}$ at a lower temperature ($\approx 550^\circ\text{C}$) with a high growth rate ($\approx 1.0 \text{ \AA/s}$) [4, 7].

Several studies have been conducted over the last few years on semiconductors based on group-III nitrides. By selecting a proper bandgap, the conversion efficiency of more than 50% can be obtained from an InGaN multijunction solar cell [9, 10]. Multijunction solar cells have several constraints, for instance, lattice mismatch between layers, controlling dislocations, thickness of layers with graded composition as well as residual strain effects, etc. [11–14]. Zhang [15] and Mesrane [16] designed and simulated an $\text{In}_{0.65}\text{Ga}_{0.35}\text{N}$ and $\text{In}_{0.622}\text{Ga}_{0.378}\text{N}$ -based single junction and an $\text{In}_{0.622}\text{Ga}_{0.378}\text{N}$ p - n -based single junction solar cell. They computed the photovoltaic parameters of the cell structure for the optimum performance. The computed efficiency was 20 to 24.2%. Shen and his group [17] obtained a similar kind of a solar cell of $\text{In}_{0.65}\text{Ga}_{0.35}\text{N}$ with a slightly higher efficiency of 24.95% by using the density of states (DOS) model. This model provides more information about the recombination/generation in semiconductors than the lifetime model by neglecting the effect of defects. The conversion efficiency of an InGaN-based solar cell calculated by Bouzid and Ben Machiche [18], for an indium fraction

($x = 0.53$), has reached 24.88%. It was then further improved [19] and an efficiency of 25.16% was attained. Akter [6] reported a 25.02% conversion efficiency from an InGaN single junction solar cell with a 1.34 eV bandgap. Benmoussa reported a 23% efficiency from an $\text{In}_{0.52}\text{Ga}_{0.48}\text{N}$ single junction solar cell with a total thickness of 830 nm [14].

A multi-layered thin-film solar cell is a second generation solar cell [20, 21] and a preliminary analysis of the parameters impeding the efficiency of the $\text{In}_x\text{Ga}_{1-x}\text{N}$ -based photovoltaic device demonstrated the chief novelty of this scientific discovery. Therefore, the aim of this work is to simulate the maximum conversion efficiency of an $\text{In}_x\text{Ga}_{1-x}\text{N}$ -based thin-film solar cell structure with the best junction configurations and parameters. The effects of the doping concentration and thickness of each layer on the electrical parameters, such as the short circuit current density J_{sc} , the open circuit voltage V_{oc} , the fill factor FF and the conversion efficiency η , have been investigated and reported here.

2. Description of simulation parameters

In this study, a thin-film solar cell structure based on $\text{In}_x\text{Ga}_{1-x}\text{N}$ has been modelled and simulated to study its physical and electrical parameters by SCAPS software. Solar Cell Capacitance Simulator (SCAPS) is a software used to simulate one-dimensional solar cells developed by the Department of Electronic and Computer Systems (ELIS), University of Gent in Belgium. Several researchers have contributed to the development of this software. This package is available free of charge to the photovoltaic (PV) research community (institutes and research establishments) [22–24].

2.1. Simulation parameters

The parameters of an $\text{In}_x\text{Ga}_{1-x}\text{N}$ -based solar cell are defined from the following equations [16, 25–27]:

- Gap energy [eV]:

$$E_g (eV) = xE_g (\text{InN}) + (1-x)E_g (\text{GaN}) - 1.43x(1-x). \quad (1)$$

The band gap value is 0.7 eV for InN and 3.42 eV for GaN at room temperature.

- Dielectric permittivity [eV]:

$$\varepsilon = x\varepsilon (\text{InN}) + (1-x)\varepsilon (\text{GaN}), \quad (2)$$

where the dielectric permittivity has the value of 15 eV for InN and 9 eV for GaN.

- Electronic affinity [eV]:

$$\chi = x\chi (\text{InN}) + (1-x)\chi (\text{GaN}), \quad (3)$$

where the electronic affinity values of InN and GaN are 5.6 eV and 4.1 eV, respectively.

- Density of states in the conduction band [cm^{-3}]:

$$N_c = 2.50945 \times 10^{19} \left(\frac{m_e}{m_0} \right)^{3/2} \left(\frac{T}{300} \right)^{3/2}, \quad (4)$$

- Density of states in the valence band [cm^{-3}]:

$$N_v = 2.50945 \times 10^{19} \left(\frac{m_t}{m_0} \right)^{3/2} \left(\frac{T}{300} \right)^{3/2}, \quad (5)$$

- Effective electron mass m_e :

$$m_e = 0.2 - 0.13x, \quad (6)$$

- Effective hole mass m_h :

$$m_h = 2.08 - 0.67x. \quad (7)$$

2.2. Structure of studied solar cell

The structure of $\text{In}_x\text{Ga}_{1-x}\text{N}$ has been studied by varying the value of x in the interval (0.5–1). Figure 1 shows a diagram of the $\text{In}_x\text{Ga}_{1-x}\text{N}$ -based solar cell. The solar cell is composed of three different layers: ZnO or IWO or CdO (antireflective), CdS or SnS (buffers) and the $\text{In}_x\text{Ga}_{1-x}\text{N}$ monolayer (absorber).

The values used for the calculation for the absorber, buffer (CdS, SnS) and the TCO layers are given in Table I.

3. Results and discussion

Figure 2 presents the current–voltage characteristics of $\text{In}_x\text{Ga}_{1-x}\text{N}/\text{SnS}/\text{ZnO}$ solar cells under light exposure. It has been observed that the value of J_{sc} increases and the value of V_{oc} decreases with the increase in indium concentration. However, as the content of indium approaches 80%, the J_{sc} values are reduced significantly and the V_{oc} value slightly improves. This is in good agreement with the previous studies [28]. For the indium content from 50 to 70%, the current density J_{sc} was observed to increase as a function of the indium content. When the content is between 70 and 80%, an abrupt drop in J_{sc} has been observed. When the indium content exceeds 80%, the current J_{sc} remains constant and the open circuit voltage decreases almost linearly as a function of the indium content from 50 to 70%. However, above 70%, an approximately constant value of V_{oc} has been observed.

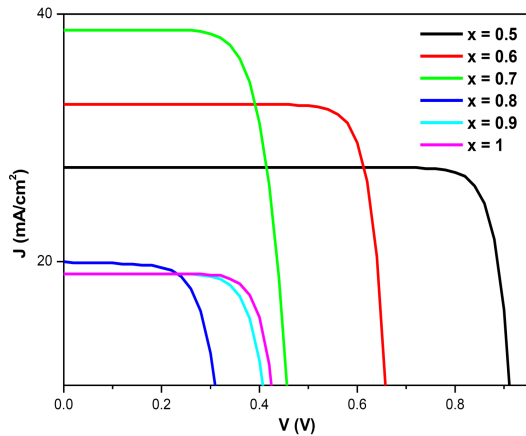
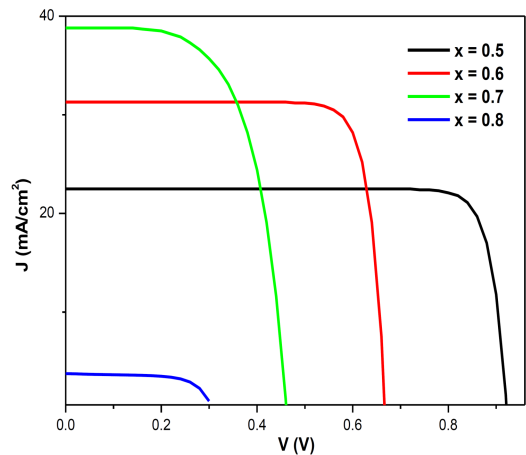
ZnO:Al	Sun  light	ZnO:Al
ZnO or IWO or CdO		
<i>0.08 μm thicker, $N_a = 10^{20} \text{ cm}^{-3}$, $N_d = 10^{14} \text{ cm}^{-3}$</i>		
CdS or SnS		
<i>0.1 μm thicker, $N_a = 10^{20} \text{ cm}^{-3}$, $N_d = 10^{14} \text{ cm}^{-3}$</i>		
$\text{In}_x\text{Ga}_{1-x}\text{N}$		
<i>4 μm thicker, $N_a = 10^6 \text{ cm}^{-3}$, $N_d = 1.5 \cdot 10^{13} \text{ cm}^{-3}$</i>		
Mo/Glass		

Fig. 1. Schematic of an $\text{In}_x\text{Ga}_{1-x}\text{N}$ -based solar cell.

Parameters of CdS, SnS and TCOs used in the simulation.

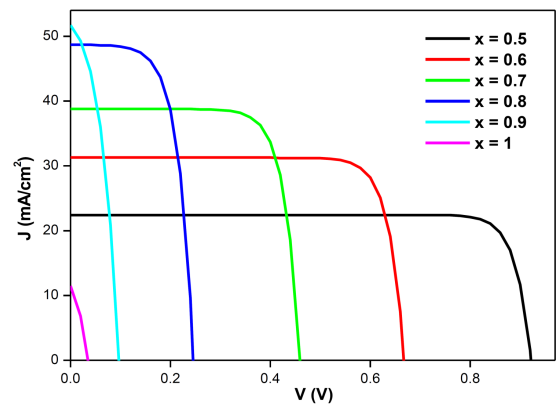
TABLE I

Parameters	CdS	SnS	ZnO	IWO	CdO
gap energy [eV]	2.45	1.25	3.4	3.7	2.2
density of states, CB N_c [cm^{-3}]	1.5×10^{18}	2×10^{18}	4×10^{18}	2.2×10^{18}	2.2×10^{18}
density of states, VB N_v [cm^{-3}]	1.8×10^{19}	1.5×10^{19}	9×10^{18}	1.8×10^{19}	1.8×10^{19}
electronic affinity [eV]	50	100	100	30	146
dielectric permittivity	20	25	25	6	29.5


Fig. 2. Influence of the concentration x on curve J - V of $\text{In}_x\text{Ga}_{1-x}\text{N}/\text{SnS}/\text{ZnO}$ structure.

Fig. 3. Influence of the concentration x on curve J - V of $\text{In}_x\text{Ga}_{1-x}\text{N}/\text{CdS}/\text{ZnO}$ structure.

The $\text{In}_x\text{Ga}_{1-x}\text{N}/\text{CdS}/\text{ZnO}$ solar cells are illuminated and the current-voltage characteristics are calculated (Fig. 3). It has been observed that — with the enhancement of the indium content — the value of J_{sc} increases, while the value of V_{oc} decreases. For 80% of the indium content, however, the value of J_{sc} has been observed to decrease significantly. The current density J_{sc} has been observed to increase for the indium content from 50 to 70% and above 80%, J_{sc} has been almost constant.

In Figure 4, we show the current-voltage characteristics of the $\text{In}_x\text{Ga}_{1-x}\text{N}/\text{In}_{0.5}\text{Ga}_{0.5}\text{N}/\text{ZnO}$ solar cells exposed to light. It is evident that the value


Fig. 4. Influence of the concentration x on curve J - V of $\text{In}_x\text{Ga}_{1-x}\text{N}/\text{In}_{0.5}\text{Ga}_{0.5}\text{N}/\text{ZnO}$ structure.

of J_{sc} increases and the value of V_{oc} decreases with the improvement of the composition, however, for a 100% indium content, J_{sc} and V_{oc} exhibit minimum values. The open circuit voltage decreases almost linearly with the increase in the indium content. For 50 to 90% of the indium content, the short-circuit current density increases but it decreases as the indium content approaches 90%.

Figure 5 represents the variation in the efficiency η as a function of the indium concentration. It has been observed that, from 10% to 50% of the indium concentration, the efficiency η increases almost linearly with the increase in the indium content. The efficiency η decreases with the increase in the indium content from 50% to 80%. The material quality is reduced when x exceeds 50% which leads directly to a higher loss of the photogenerated charge carriers. Above the 80% concentration of indium, the efficiency value remains almost constant. Our results are in agreement with those already published [29, 30].

By changing the TCO by IWO or CdO with the buffer layer SnS, the best yields have been achieved as a function of the indium content. The J - V curves under illumination obtained for different concentrations of the $\text{In}_x\text{Ga}_{1-x}\text{N}/\text{SnS}/\text{IWO}$ and $\text{In}_x\text{Ga}_{1-x}\text{N}/\text{SnS}/\text{CdO}$ structures are shown in Fig. 6.

In both cases, the short-circuit current J_{cc} increases with increasing the indium content, however, as the concentration attains the 80% value, J_{cc} approximately becomes constant. For the

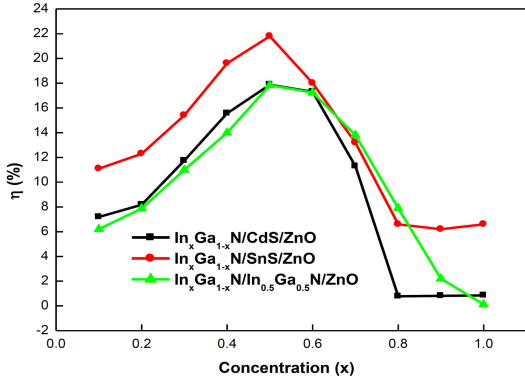


Fig. 5. The efficiency η as a function of concentration of an $\text{In}_x\text{Ga}_{1-x}\text{N}$ -based structure.

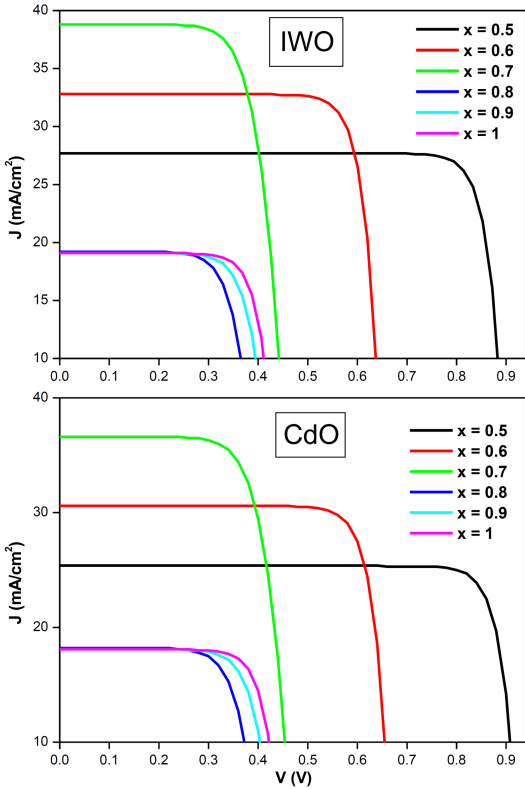


Fig. 6. The J - V curves of the $\text{In}_x\text{Ga}_{1-x}\text{N}/\text{SnS}/\text{IWO}$ and $\text{In}_x\text{Ga}_{1-x}\text{N}/\text{SnS}/\text{CdO}$ solar cells.

no-load voltage V_{oc} , for the indium content from 50 to 80%, the voltage is observed to decrease as a function of the indium content, however, it increases slightly for $\text{In}_{0.9}\text{Ga}_{0.1}\text{N}$ and for the binary compound InN .

The output parameters of the deduced cells are summarized in Table II. By enhancing the indium content in the absorbent layer and by changing the TCO, we have observed that: (i) regardless of the indium content, the no-load voltage and form factor values are almost equal for the two structures; (ii) there is a certain decrease in the current density J_{cc} for the $\text{In}_x\text{Ga}_{1-x}\text{N}/\text{SnS}/\text{CdO}$ structure

TABLE II

Output parameters of $\text{In}_x\text{Ga}_{1-x}\text{N}/\text{SnS}/\text{CdO}$ and $\text{In}_x\text{Ga}_{1-x}\text{N}/\text{SnS}/\text{IWO}$.

	$\text{In}_x\text{Ga}_{1-x}\text{N}/\text{SnS}/\text{CdO}$		$\text{In}_x\text{Ga}_{1-x}\text{N}/\text{SnS}/\text{IWO}$	
	FF [%]	η [%]	FF [%]	η [%]
$\text{In}_{0.5}\text{Ga}_{0.5}\text{N}$	86.34	20.23	86.38	22.13
$\text{In}_{0.6}\text{Ga}_{0.4}\text{N}$	82.57	16.86	82.61	18.11
$\text{In}_{0.7}\text{Ga}_{0.3}\text{N}$	72.40	12.45	72.13	13.19
$\text{In}_{0.8}\text{Ga}_{0.2}\text{N}$	73.01	5.36	73.10	5.69
$\text{In}_{0.9}\text{Ga}_{0.1}\text{N}$	75.045	5.87	75.08	6.23
InN	77.71	6.25	77.75	6.63

as compared to the second structure; (iii) the conversion efficiency of the $\text{In}_x\text{Ga}_{1-x}\text{N}/\text{SnS}/\text{IWO}$ cells is higher than that of the $\text{In}_x\text{Ga}_{1-x}\text{N}/\text{SnS}/\text{CdO}$ cells, with a difference between 0.33 and 1.9.

4. Conclusion

Solar cells based on $\text{In}_x\text{Ga}_{1-x}\text{N}$ with several affordable innovative structures have been simulated using the SCAPS package. The effect of variation in the indium content on the electrical characteristics of the cell, such as the open circuit voltage V_{oc} , the short circuit current density J_{sc} , the form factor FF and the conversion efficiency η , have been investigated. The influence of the SnS, CdS, $\text{In}_{0.5}\text{Ga}_{0.5}\text{N}$ buffer layer on the $\text{In}_x\text{Ga}_{1-x}\text{N}/\text{SnS}/\text{ZnO}$ structure and the effect of the TCO layer on the electrical characteristics of the structure are also measured. It is observed that the short circuit current J_{cc} increases with the increase in the indium content, however, as the concentration attains the 80% value, J_{cc} approximately becomes constant. For the no-load voltage V_{oc} and for the indium content from 50 to 80%, the voltage is observed to decrease as a function of the indium content, however, it slightly increases for $\text{In}_{0.9}\text{Ga}_{0.1}\text{N}$ and the binary compound InN . The effects of doping concentration and thickness of each layer on the electrical parameters of the $\text{In}_x\text{Ga}_{1-x}\text{N}$ alloys indicate that these alloys are promising candidates for thin-film solar cells.

References

- [1] A. Khettou, I. Zeydi, M. Chellali, M. Ben Arbia, S. Mansouri, H. Helal, H. Maaref, *Superlatt. Microstruct.* **142**, 106539 (2020).
- [2] A. Aissat, J. Vilcot, *Optik* **207**, 163844 (2020).
- [3] M. Hori, K. Kano, T. Yamaguchi, Y. Satto, T. Araki, Y. Nanishi, N. Teraguchi, A. Suzuki, *Phys. Status Solidi B* **234**, 750 (2002).
- [4] D.V.P. McLaughlin, J.M. Pearce, *Metall. Mater. Trans. A* **44**, 1947 (2013).

- [5] Y. Marouf, L. Dehimi, F. Bouzid, F. Pezzimenti, F.G. Della Corte, *Optik* **163**, 22 (2018).
- [6] N. Akter, *Int. J. Res. Eng. Technol.* **3**, 315 (2014).
- [7] C.F. Huang, W.Y. Hsieh, B.C. Hsieh, C.H. Hsieh, C.F. Lin, Chia-Feng, *Thin Solid Films* **529**, 278 (2013).
- [8] H. Ekinici, V.V. Kuryatkov, C. Forgey, A. Dabiran, R. Jorgenson, S.A. Nikishin, *Acta Phys. Pol. A* **135**, 759 (2019).
- [9] D.N. Papadimitriou, *Appl. Sci.* **10**, 232 (2020).
- [10] U.K. Kumawat, A. Das, K. Kumar, A. Dhawan, *Opt. Expr.* **28**, 11806 (2020).
- [11] Yuji Zhao, Xuanqi Huang, Houqiang Fu, Hong Chen, Zhijian Lu, J. Montes, I. Baranowski, in: *Proc. 2017 IEEE 60th Int. Midwest Symp. on Circuits and Systems (MWSCAS), Boston (MA)*, 2017, p. 954.
- [12] G. Ali, M. Omar, M.F.N. Khan, M. Iqbal, in: *Proc. 2018 Int. Conf. on Computing, Mathematics and Engineering Technologies (iCoMET)*, Sukkur, 2018, p. 1.
- [13] J. Li, F. Li, S. Lin et al., *Proc. SPIE* **7409**, 740910 (2009).
- [14] D. Benmoussa, B. Hassane, H. Abderrachid, in: *Proc. 1st Int. Renewable and Sustainable Energy Conf. (IRSEC '13), Ouarzazate (Morocco), 2013*, IEEE, 2013, p. 23.
- [15] X. Zhang, X. Wang, H. Xiao, C. Yang, J. Ran, C. Wang, Q. Hou, J. Li, *J. Phys. D* **40**, 7335 (2007).
- [16] A. Mesrane, F. Rahmoune, A. Mahrane, A. Oulebsir, *Int. J. Photoenergy* **2015**, 594858 (2015).
- [17] X. Shen, S. Lin, F. Li, et al., *Proc. SPIE* **7045**, 70450E (2008).
- [18] F. Bouzid, S. Ben Machiche, *Rev. Energ. Renouvelabl.* **14**, 47 (2011).
- [19] F. Bouzid, L. Hamlaoui, *J. Fundament. Appl. Sci.* **4**, 59 (2012).
- [20] B. Zaidi, C. Shekhar, B. Hadjoudja, S. Gagui, B. Chouial, *Acta Phys. Pol. A* **136**, 495 (2019).
- [21] B. Zaidi, M. Zouagri, S. Merad, C. Shekhar, B. Hadjoudja, B. Chouial, *Acta Phys. Pol. A* **136**, 988 (2019).
- [22] M. Burgelman, P. Nollet, S. Degrave, *Thin Solid Films* **361**, 527 (2000).
- [23] K. Decock, S. Khelifi, M. Burgelman, *Thin Solid Films* **519**, 7481 (2011).
- [24] M. Burgelman, J. Verschraegen, S. Degrave, P. Nollet, *Prog. Photovolt. Res. Appl.* **12**, 143 (2004).
- [25] M. Anani, C. Mathieu, M. Khadraoui, Z. Chama, S. Lebid, Y. Amar, *Microelectron. J.* **40**, 427 (2009).
- [26] J.W. Ager, N. Miller, R.E. Jones, K.M. Yu, J. Wu, W.J. Schaff, W. Walukiewicz, *Phys. Status Solidi B* **245**, 873 (2008).
- [27] S.J. Pearton, J.C. Zolper, R.J. Shul, F. Ren, *Appl. Phys.* **86**, 1 (1999).
- [28] S. Lin, X. Li, H. Pan, H. Chen, X. Li, Y. Li, J. Zhou, *Energy Convers. Manage.* **119**, 361 (2016).
- [29] M.R. Islam, M.A. Rayhan, M.E. Hosain, A.G. Bhuiyan, M.R. Islam, A. Yamamoto, in: *Proc. Int. Conf. on Electrical and Computer Engineering, Dhaka (Bangladesh), 2006*, p. 241.
- [30] I. Ul Islam Chowdhury, J. Sarker, A.S.M. Zadid Shifat, R.A. Shuvro, A.F. Mitul, *Results Phys.* **9**, 432 (2018).